

Supersymmetric hadronic bound state detection at e^+e^- colliders

M. Antonelli*

INFN Milano and

Milano University , via Celoria 16, Milano, Italy

N. Fabiano†

INFN National Laboratories, P.O.Box 13, I00044 Frascati, Italy

Abstract

We review the possibility of formation for a bound state made out of a stop quark and its antiparticle. The detection of a signal from its decay has been investigated for the case of a e^+e^- collider.

*Mario.Antonelli@lnf.infn.it

†Nicola.Fabiano@lnf.infn.it

1 Introduction

In the Standard Model it has been verified that there is creation of bound states for every quark but the top (see for instance [1, 2, 3, 4, 5] and references therein). The latter possibility is ruled out due to the high value of the top quark mass, which is responsible for its short lifetime. The natural step forward would be to consider the possibility of bound states creation outside the Standard Model. In this case we focus our attention to the supersymmetric extensions of the Standard Model [6], in particular to the resonant production [7, 8] and detection of a bound state (supermeson) created from a stop and an anti-stop (“stoponium”) at e^+e^- colliders.

2 Bound States

In this Section we will review the bound states creation. For the SUSY case, our assumption will be that the bound state creation does not differ from the SM case, as the relevant interaction is again driven by QCD, and is regulated by the mass of the constituent (s)quarks.

A formation criterion states that [5] the formation of a hadron can occur only if the level splitting between the lying levels of the bound states, which depend upon the strength of the strong force between the (s)quarks and their relative distance [4], is larger than the natural width of the state. It means that, if

$$\Delta E_{2S-1S} \geq \Gamma \tag{1}$$

where $\Delta E_{2S-1S} = E_{2S} - E_{1S}$, Γ is the width of the would-be bound state, then the bound state exists.

For the case of a scalar bound state $\bar{t}t$, without referencing to a particular supersymmetric model, we should consider the Coulombic two-body interaction

$$V(r) = -\frac{4}{3} \frac{\alpha_s}{r} \tag{2}$$

with the two-loop expression for α_s [9]

$$\alpha_s(Q^2) = \frac{4\pi}{\beta_0 \log \left[Q^2 / \Lambda_{\overline{MS}}^2 \right]} \left\{ 1 - \frac{2\beta_1}{\beta_0^2} \frac{\log \left[\log \left[Q^2 / \Lambda_{\overline{MS}}^2 \right] \right]}{\log \left[Q^2 / \Lambda_{\overline{MS}}^2 \right]} \right\} \tag{3}$$

with $\beta_0 = 11 - \frac{2}{3} n_f$, $\beta_1 = 51 - \frac{19}{3} n_f$. Due to the present limits on the stop mass [10, 11] we could either assume that the stop is lighter than the top quark, that is $n_f = 5$, or heavier, i.e. $n_f = 6$. The α_s expression (3) has to be evaluated at a fixed scale $Q^2 = 1/r_B^2$, where r_B is the Bohr radius

$$r_B = \frac{3}{4\mu\alpha_s} \tag{4}$$

and μ is the reduced mass of the system. It has been shown in [5, 4] that in the case of high quark mass values, the predictions of the Coulombic potential evaluated at this scale do not differ from the other potential model predictions.

In figures 1 and 2 we show a plot of the energy splitting for the first two levels of the stoponium bound state with respect to the stop mass, for the LHC and the NLC case respectively. As from (1), those figures have to be compared to the width of the stoponium. The width of the stoponium, $\Gamma_{\tilde{t}\tilde{t}}$, is twice the width of the single stop squark, as each should decay in a manner independent from the other.

There are several ways a stop should decay [12], depending on the assumptions made for the other superpartners. For very low values of the stop quark mass, the highest width value will not exceed a few KeV , quite smaller than the energy splitting of the first two levels of the stoponium. As the mass increases more decay modes enter in and the width increases. In particular for the regime where $m_W + m_{\tilde{\chi}^0} + m_b < m_{\tilde{t}} < m_{\tilde{\chi}^+} + m_b$ the three body decay $\tilde{t} \rightarrow bW\tilde{\chi}^0$ is kinematically allowed and is comparable to the flavour changing two body decay $\tilde{t} \rightarrow c\tilde{\chi}^0$ [13]. Here $\tilde{\chi}^0$ refers to the lightest supersymmetric particle (LSP); $\tilde{\chi}^+$ is the lightest chargino. Even in this case those widths do not exceed values in the KeV range. In this scenario we see, as before, that the energy splitting is much larger than the decay width of the bound state, thus hadronization is possible.

For even higher stop masses, the picture changes [14] as more two body decays like $\tilde{t} \rightarrow b\chi^+$ and $\tilde{t} \rightarrow t\tilde{\chi}^0$ are available. For these values of the stop mass there are regions of the parameter space where the decay widths, even if lowered by the one-loop corrections [14], could overtake the energy levels splitting, thus jeopardizing the formation of the supersymmetric bound state. For instance, in the region where $\mu \sim M_2$ the decay width would be larger than ΔE_{2S-1S} for stop masses of about $200 GeV$, spoiling hadronization for $m_{\tilde{t}}$ beyond this range (here μ is the Higgs-higgsino mass parameter, while M_2 is the wino mass parameter). On the contrary, for parameter values where $\mu \ll M_2$, the decay width of those modes are substantially lower. This would allow stoponium formation for stop mass values in the energy range of the future NLC collider. The region where $\mu \gg M_2$ is in a situation intermediate between the two described above.

A quantitative description of the stoponium formation could be seen in figures (3) and (4), where we report the regions of the $\mu - M_2$ plane for two values of $\tan\beta$ in which stoponium cannot be formed, as a function of the stop mass.

Regarding the hadronization problem we see that there are many possibilities due to the vast parameter space. For stop mass values under about $100-200 GeV$ and $\tan\beta = 1.5$ there is a window of opportunity for stoponium formation regardless of the parameter values; beyond that range the stoponium formation would either be allowed or forbidden depending upon the choice of the parameters.

3 Cross Section and Decay Width

The next natural step would be to see whether the stoponium could be detected on an e^+e^- collider with LEP or future NLC characteristics. For this purpose we shall calculate its cross section and decay modes; basing our predictions on [15], and updating their results.

We should look for the production and decay of the P wave state, since we are interested in the search of the bound state at a e^+e^- collider, conserving thus quantum numbers.

We use the Breit–Wigner formula to evaluate the total cross section [10]:

$$\sigma = \frac{3\pi}{M^2} \times \frac{\Gamma_e \Gamma_{tot}}{(E - M)^2 + \Gamma_{tot}^2/4} \quad (5)$$

where M is the mass of the resonance, E is the centre-of-mass energy, Γ_{tot} is the total width, and Γ_e is the decay width to electrons.

The first decay we will investigate is the leptonic one, which is given by the Van Royen–Weisskopf formula [16]

$$\Gamma(2P \rightarrow e^+ e^-) = 24\alpha^2 Q^2 \frac{|R'(0)|^2}{M^4} \quad (6)$$

$R'(0)$ is the derivative of the radial wavefunction calculated at the origin, M the mass of the bound state, α the QED constant, Q the (s)quark charge. In this case we are neglecting the stop coupling to the Z boson, and this allows to hide into the total width all the dependencies of the MSSM parameters for the cross-section formula (5).

For this and following cases, we shall make use of the radial wavefunctions of the Coulombic model, as presented in Section (1). Those are, for the $1S$ state

$$R_{1S}(r) = \left(\frac{2}{r_B}\right)^{3/2} \exp\left(-\frac{r}{r_B}\right) \quad (7)$$

and for the $2P$

$$R_{2P}(r) = \frac{1}{\sqrt{3}} \left(\frac{1}{2r_B}\right)^{3/2} \frac{r}{r_B} \exp\left(-\frac{r}{2r_B}\right) \quad (8)$$

r_B is the Bohr radius defined in (4).

For the hadronic width decay we have the following expression

$$\Gamma(2P \rightarrow 3g) = \frac{64}{9} \alpha_s^3 \frac{|R'(0)|^2}{M^4} \log(m_{\bar{t}} r_B) \quad (9)$$

where the Bohr radius acts as an infrared cutoff [15].

The $2P$ state could also decay into a $1S$ state and emit a photon. The width decay in this case is given by

$$\Gamma(2P \rightarrow 1S + \gamma) = \frac{4}{9} \alpha Q^2 (\Delta E_{2S-1S})^3 D_{2,1} \quad (10)$$

where ΔE_{2S-1S} is the energy of the emitted photon, and $D_{2,1} = \langle 2P|r|1S \rangle$ is the dipole moment [17]. In figures 5 and 6 we present the decays of the $2P$ state into hadrons and into a $1S$ state plus a photon as a function of the stop mass, as predicted by the Coulombic model. In this case the behaviour of the hadronic decay width with respect to the stop mass is $\Gamma(2P \rightarrow 3g) \sim m\alpha_s^8$, while the radiative decay width goes like $\Gamma(2P \rightarrow 1S + \gamma) \sim m^2\alpha_s^5$. In the former case the linear growth with m is suppressed by the high power of α_s , resulting in an essentially constant width for the stop mass range of our interest. The $3g$ width will eventually grow faster for stop mass values larger than about 1 TeV . The behaviour of the $2P \rightarrow 1S + \gamma$ decay is more straightforward, since it grows faster with m and contains a lower power of α_s . It is also apparent that among the two the $2P \rightarrow 1S + \gamma$ decay width dominates for increasing

values of the stop mass as it is clearly seen in figure 5 and particularly in 6. It is possible to notice also a small threshold effect due to the inclusion of the top flavour.

We must point out that this behaviour of decay widths of the stop bound state is given by the particular Coulombic potential model used in the computation. The results obtained however do not lose validity because, as it has been shown in [2, 4, 5], this Coulombic model does not differ significantly from other more popular potential models when the mass of the constituent (s)quarks gets larger. This fact could be intuitively understood by considering the Bohr radius of the bound state, which decreases like $1/m$: therefore the constituent (s)quarks “feel” more and more the Coulombic part of the potential which becomes dominant with respect to other components of the potential, like for instance the linear confining term that is added in the description of mesons containing lighter quarks.

For a light stop the analysed annihilation modes are the dominant widths [12] so far. As the stop mass increases the single stop decay modes will dominate the total width because of the opening of the decay channel $\tilde{t} \rightarrow t\tilde{\chi}^0$ and $\tilde{t} \rightarrow b\tilde{\chi}^+$.

Figure 7 shows the peak cross section obtained from (5) as function of the stop mass for 200 GeV center of mass energy (LEP2). The evaluation of the peak cross-section assumes that the annihilation modes are dominant. While the peak cross section is in the nb range, the resonance is practically undetectable at the present collider because its width is much smaller than the typical beam energy spread (of the order of 200 MeV at LEP2 [10]). The effect of a growth of the total width – due to e.g. the opening of other decay channels [18] – does not change the result, as the net effect will be a decrease of the peak cross section. This is clearly illustrated in figure 8 where the Breit–Wigner formula (5) is folded with the typical energy spread of the beam of 200 MeV.

The possibility of stoponium production with radiative returns has also been considered and the results for the cross-sections are illustrated in figure (9). We see that the cross-section is quite small, and in this manner there is no possibility of seeing any signal.

With the increase of the centre of mass energy (NLC case) the scenario changes: as more decay channels appear there are regions in the parameter space where the stoponium could not be formed. The net result for the signal detection does not change, as it could clearly be seen in figures (10) and (11) where we show the effective total cross-section and the radiative return cross-section for centre of mass energy of 500 GeV.

4 Conclusions

We have shown that because of the high energy binding and of the narrow decay width the formation of a $\tilde{t}\tilde{t}$ P wave bound state is possible in certain regions of the parameter space, and in particular for a light stop. However our result shows that this supersymmetric bound state cannot be detected at the present and even future e^+e^- collider. The latter fact proves also that it gives a negligible contribution to the $\tilde{t}\tilde{t}$ production cross section.

Acknowledgments

We Thank G. Pancheri for useful discussion and suggestions. We would like to thank also

G. Altarelli and V. Khoze for careful reading of the manuscript. One of us (N.F.) wishes to thank A. Masiero for useful discussion.

References

- [1] V.S. Fadin, V.A. Khoze, *JETP Lett.* **46** (1987) 525;
V.S. Fadin, V.A. Khoze, *Yad. Fiz.* **48** (1988) 487;
I. Bigi, V.S. Fadin, V.A. Khoze, *Nucl. Phys* **377B** (1992) 461.
- [2] G. Pancheri, J.P. Revol and C. Rubbia, *Phys. Lett.* **B277** (1992) 518.
- [3] J.H. Kühn, E. Mirkes, *Phys. Lett.* **B296** (1992) 425;
J.H. Kühn, E. Mirkes, *Phys. Rev.* **D48** (1993) 179.
- [4] N. Fabiano, *Eur. Phys. J.* **C2** 345 (1998).
- [5] N. Fabiano, A. Grau and G. Pancheri, *Phys. Rev.* **D50** (1994) 3173;
“*Toponium from different potential models*”, *Nuovo Cimento A*, Vol 107, 2789,(1994).
- [6] For a review see:
Ed. M. Jacob, *Supersymmetry and Supergravity*.
- [7] M. Drees, M. Nojiri, *Phys.Rev.* **D49** (1994) 4595.
- [8] W. Mödritsch, *Phys.Lett.* **B349** (1995) 525.
- [9] W.A. Bardeen, A.J. Buras, D.W. Duke and T. Muta, *Phys. Rev.* **D18** (1978) 3998;
W.J. Marciano, *Phys. Rev.* **D29** (1984) 580.
- [10] Review of Particle Properties, *EuroPhys. Journ.* **C3** (1998) 1;
<http://pdg.lbl.gov/>
- [11] ALEPH Collaboration, *Search for Scalar Top and Scalar Bottom Quarks at LEP2*, *Phys. Lett.* **B 413** (1997) 431;
Search for Light Top Squarks in $p\bar{p}$ Collisions at $\sqrt{s} = 1.8$ TeV, *Phys. Rev. Lett.* **76** (1996) 2222;
OPAL Collaboration, *Search for Scalar Top and Scalar Bottom Quarks at $\sqrt{s} = 170$ GeV - 172 GeV in $e^+ e^-$ Collisions*, *Z. Phys.* **C 75** (1997) 409.
- [12] K. Hikasa and M. Kobayashi, *Phys. Rev.* **D36** (1987) 724.
- [13] W.Porod and T. Wöhrmann, *Phys. Rev.* **D55** (1997) 2907.
- [14] A. Djouadi, W. Hollik and C. Jünger, *Phys. Rev.* **D55** (1997) 6975; see also references therein.
- [15] C. Nappi, *Phys. Rev.* **D25** (1982) 84.
- [16] R.Van Royen and V.Weisskopf, *Nuovo Cimento* **50A** (1967) 617.

- [17] J. Kühn and P.M. Zerwas, *Phys. Rev.* **167** (1988) 321.
- [18] A. Bartl et al., *Phys. Lett.* **B384** (1996) 151; *Z. Phys.* **C73** (1997) 469.
- [19] Ed. R. Brinkmann, G. Materlik, J. Rossbach, A. Wagner, *Conceptual Design of a 500 GeV e^+e^- Linear Collider with Integrated X-Ray Laser Facility*, Vol. 1 (1997);
Ron Settles, private communication;
Marcello Piccolo, private communication.

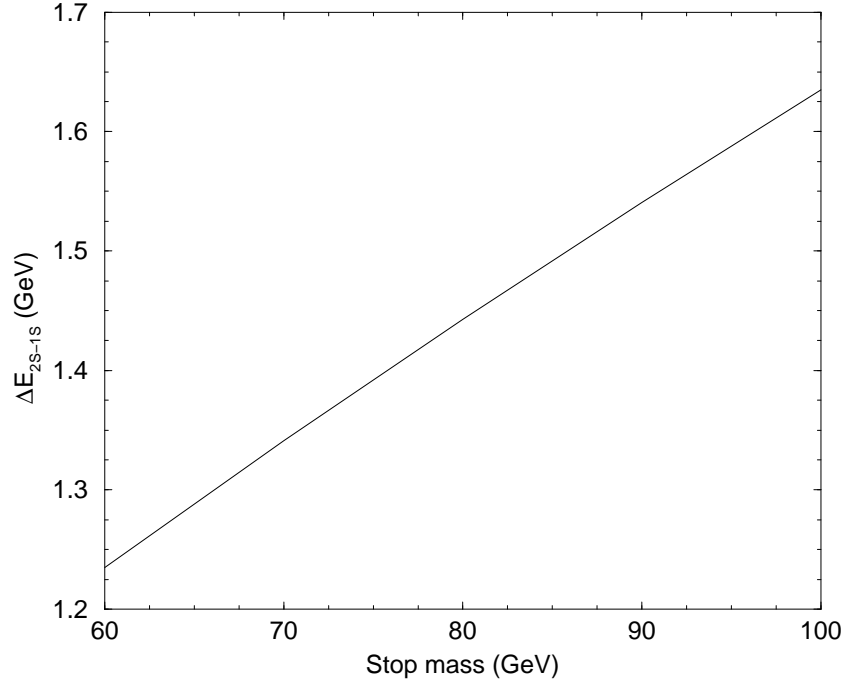


Figure 1: ΔE_{2S-1S} as a function of the stop mass up to 100 GeV for the Coulombic model.

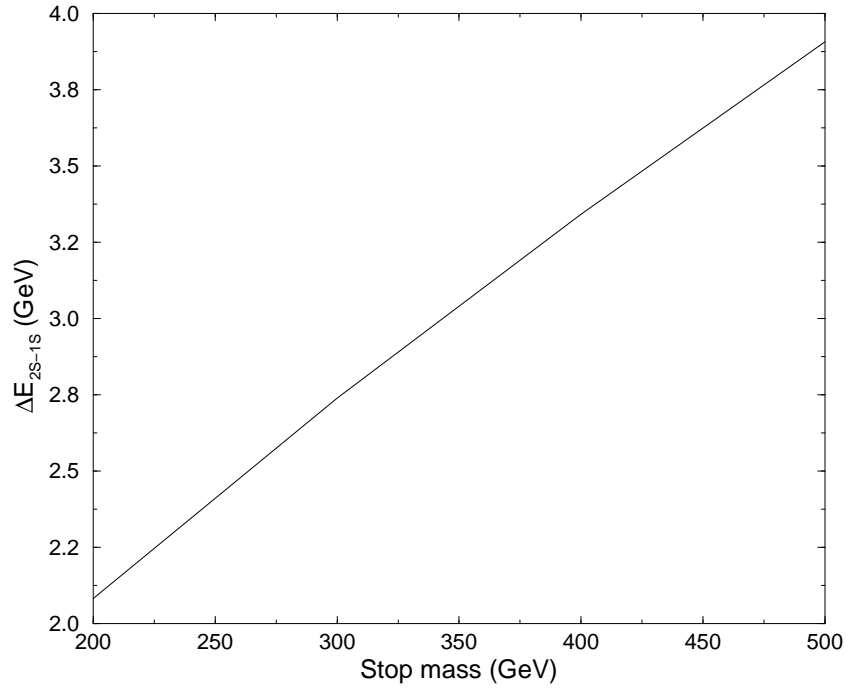


Figure 2: ΔE_{2S-1S} as a function of the stop mass up to 500 GeV for the Coulombic model.

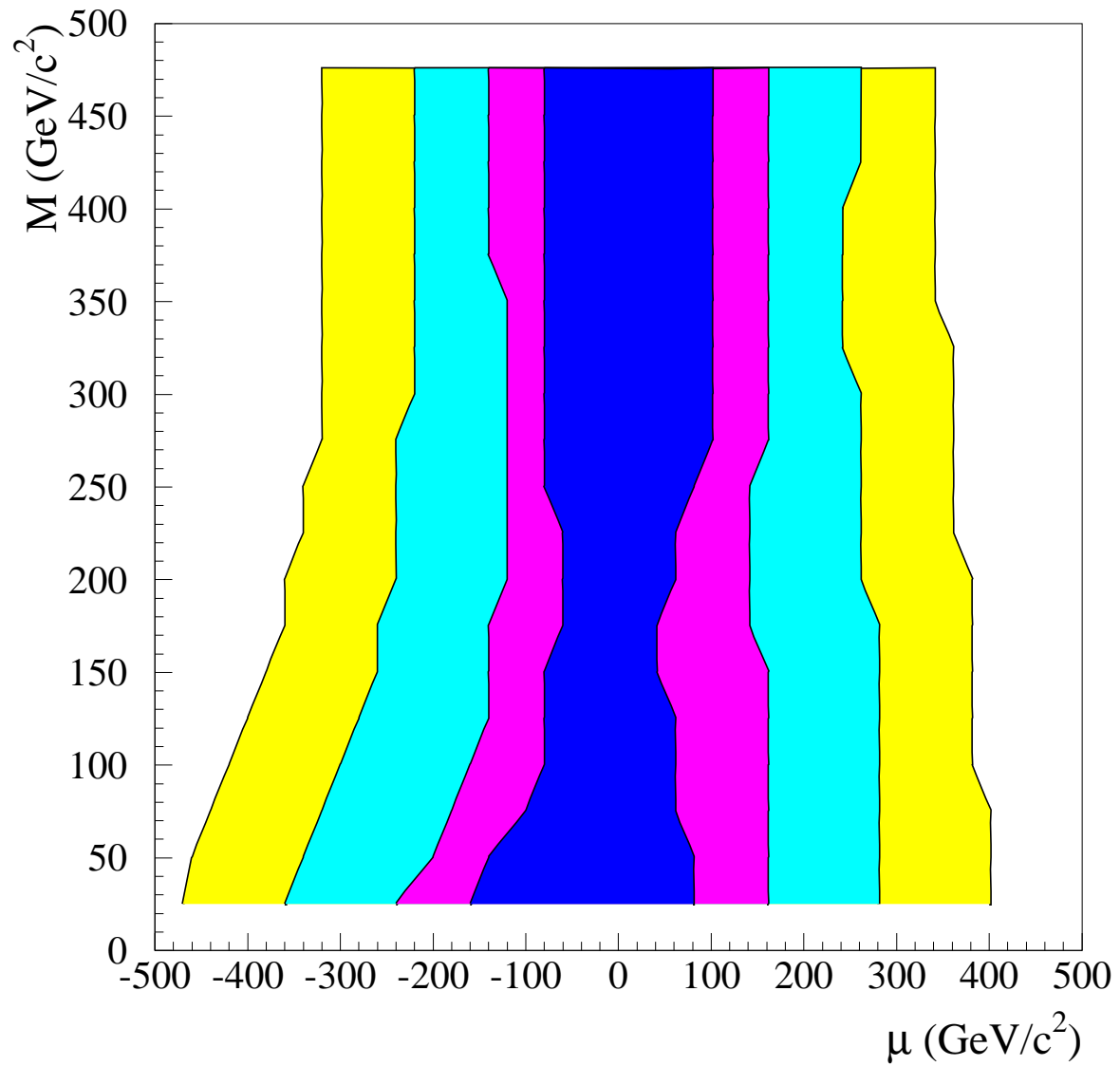


Figure 3: *Regions in the $\mu - M_2$ plane where stoponium formation is forbidden ; $\tan \beta = 1.5$. The different colours refer to various values of the stop mass: 250, 300, 400 and 500 GeV respectively, in increasing brightness.*

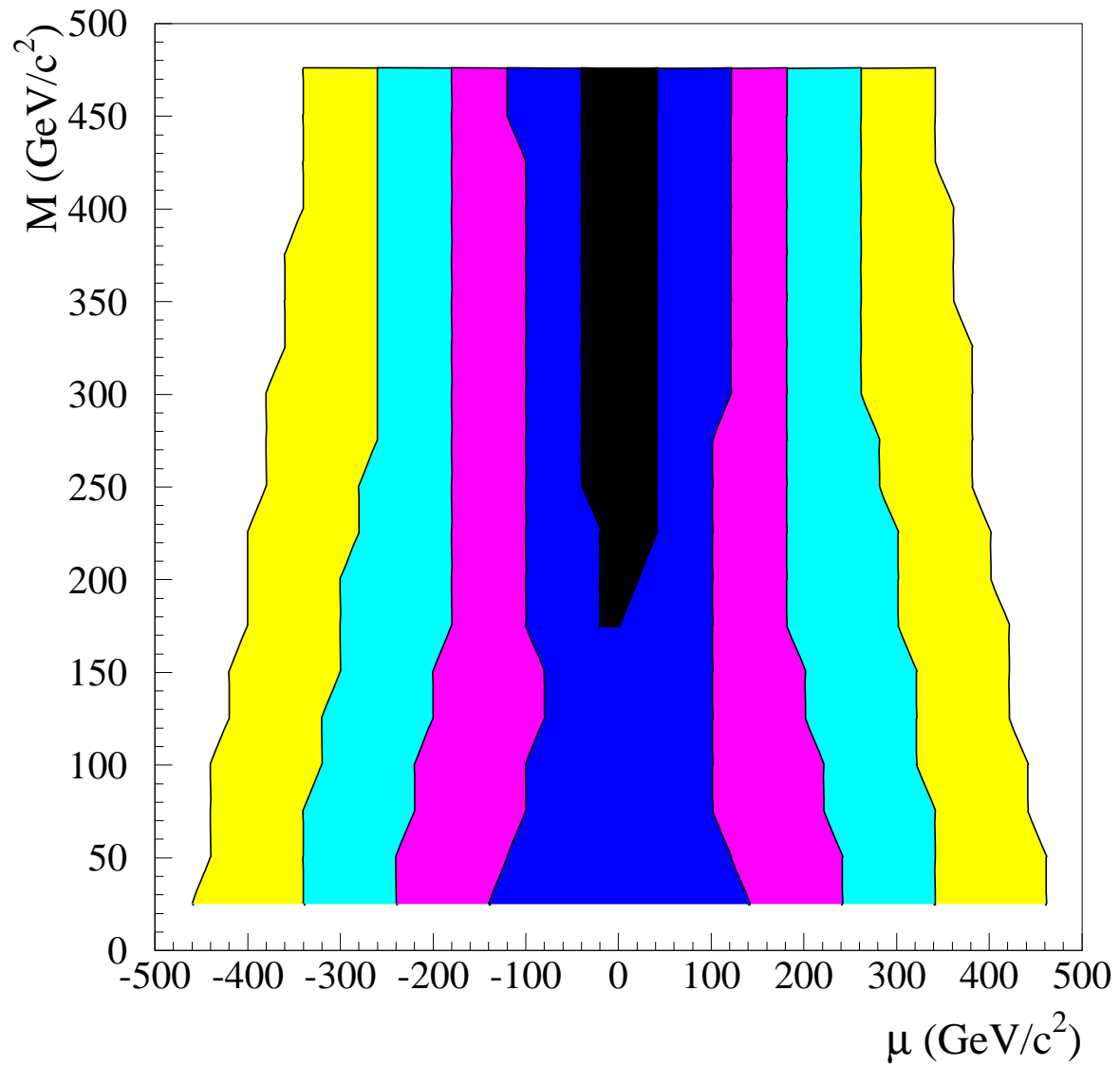


Figure 4: *Regions in the $\mu - M_2$ plane where stoponium formation is forbidden ; $\tan \beta = 40$. The different colours refer to various values of the stop mass: 100, 200, 300, 400 and 500 GeV respectively, in increasing brightness.*

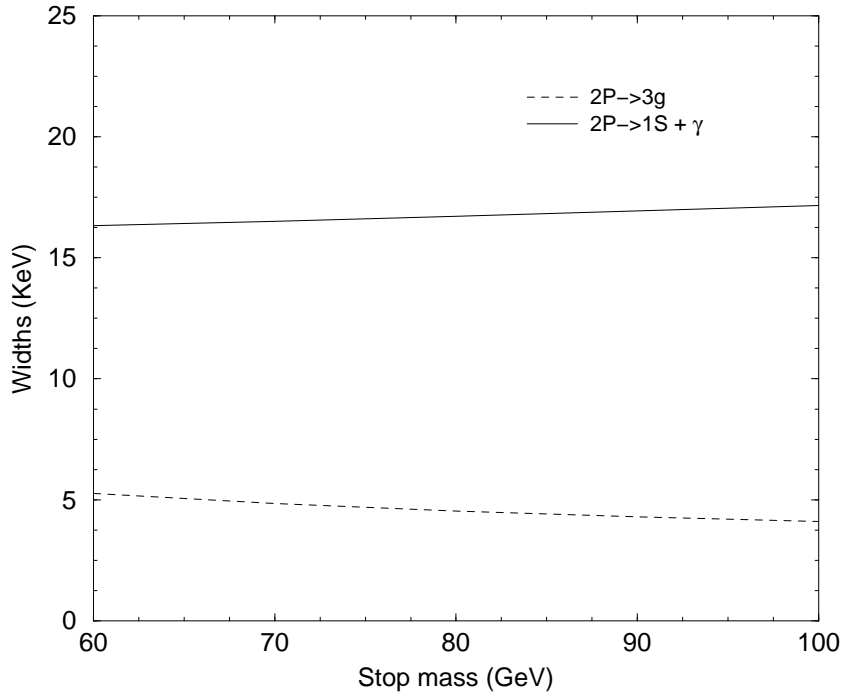


Figure 5: *Decay widths for the 2P state with respect to the stop mass for the Coulombic model. The dashed line represents the decay into hadrons, the continuous line the decay into the 1S state and an emitted photon.*

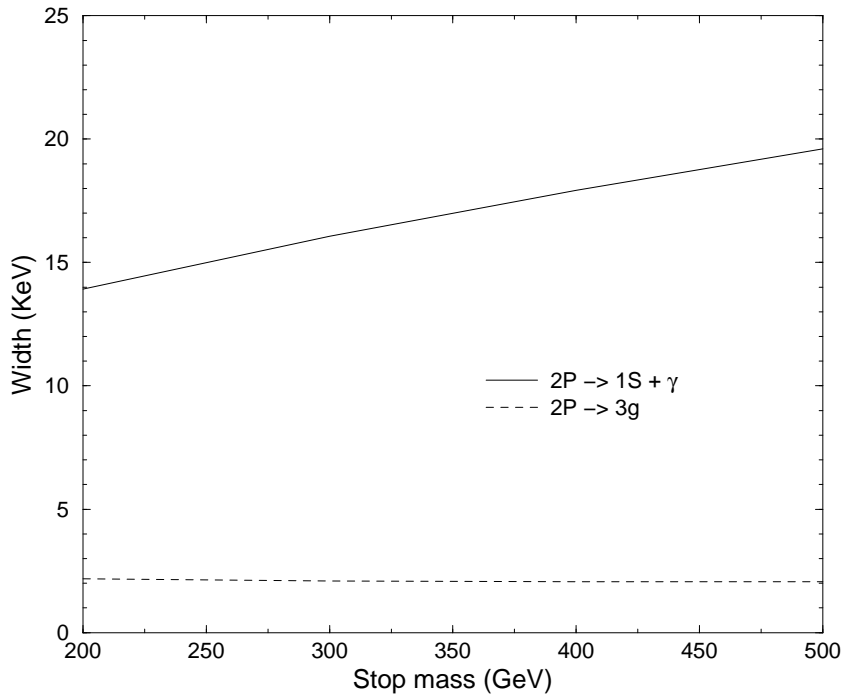


Figure 6: *Like Fig. 5, for a mass range of up to 500 GeV, for NLC.*

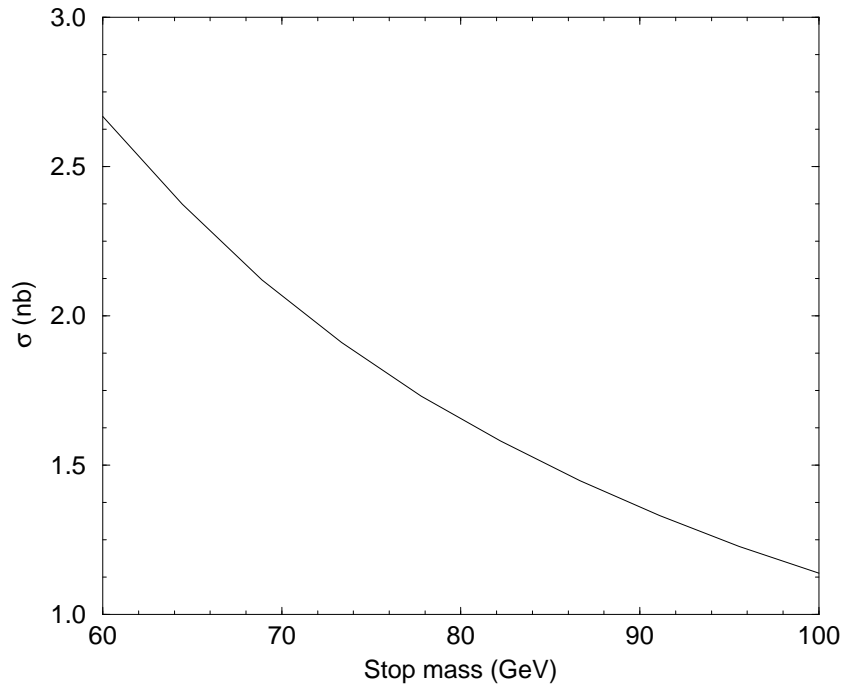


Figure 7: *Peak cross section as a function of the stop mass, for the LEP case, at Born level.*

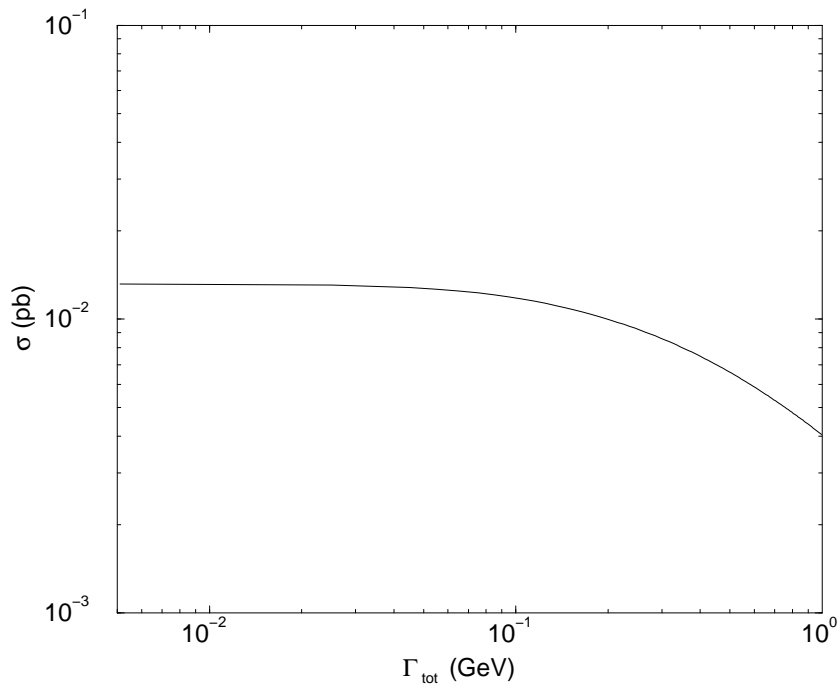


Figure 8: *Total cross section folded with a beam energy spread of 200 MeV as a function of the total width of the stop, at Born level. The plot has been obtained for a stop mass of 100 GeV.*

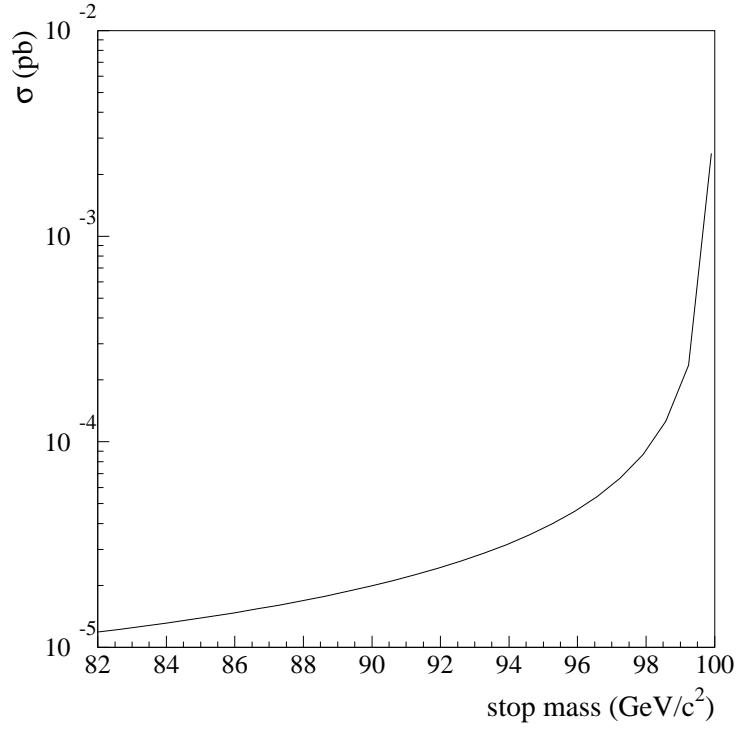


Figure 9: *Radiative return production cross section as a function of the stop mass, for the LEP case.*

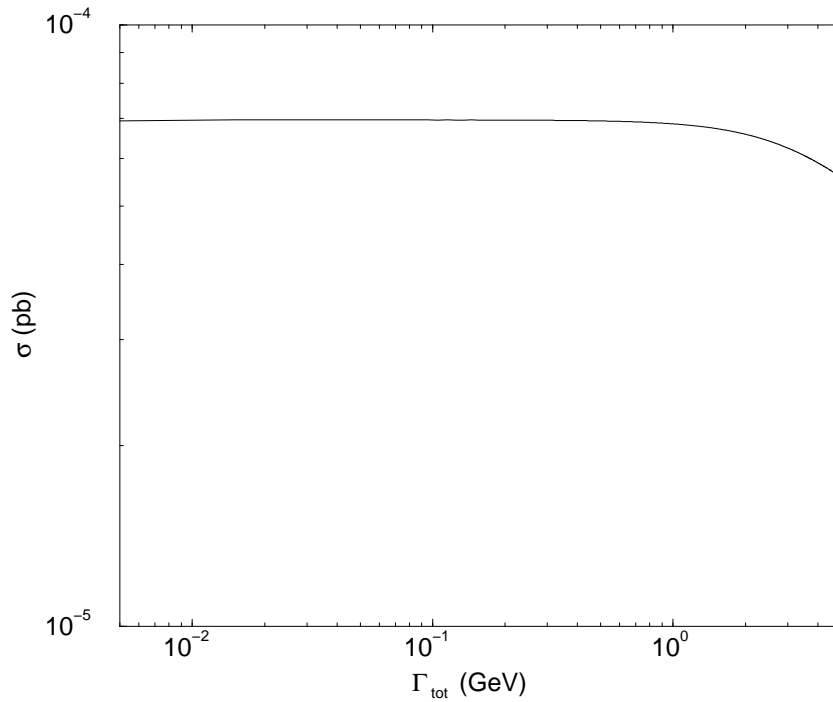


Figure 10: *Like Fig. 8, for a beam energy spread of 6 GeV (NLC) [19]. The plot has been obtained for a stop mass of 200 GeV.*

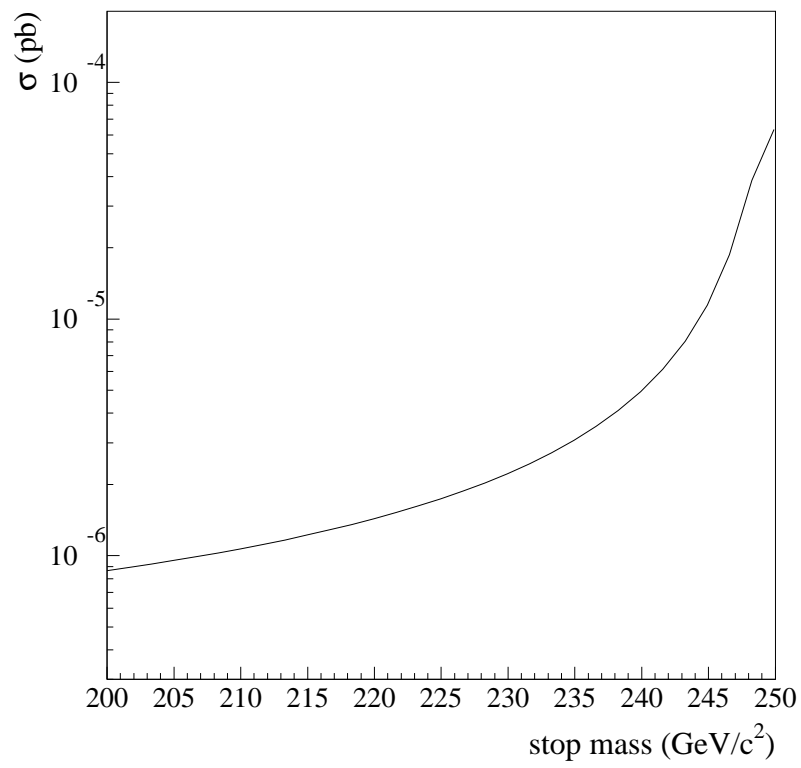


Figure 11: *Radiative return production cross section as a function of the stop mass, for the NLC case.*